COMPREHENSIVE DYNAMIC MODEL OF A CABLE-DRIVEN PARALLEL ROBOT USING THE BOND GRAPH APPROACH

Ishan Chawla and Pushparaj Mani Pathak
Indian Institute of Technology Roorkee, Roorkee-247667, India.
ichawla@me.iitr.ac.in and pushparaj.pathak@me.iitr.ac.in

Arun Kumar Samantaray
Indian Institute of Technology Kharagpur, Kharagpur-721302, India.
samantaray@mech.iitkgp.ernet.in

ABSTRACT

Cable-driven parallel robots (CDPRs) are well known for the applications requiring large workspaces. The mass and elasticity of the cable have a significant effect on the dynamics of large-scale CDPRs. However, most of the work in literature assume the cable to be massless and inelastic for the dynamic modeling. Therefore, this paper proposes a comprehensive dynamic model of the cable-driven parallel robot which takes the cable mass, elasticity, flexural stiffness, flexural damping and cable-pulley interaction into consideration. The modeling is done by considering the cable as a series of spring-mass-damper systems connected by the revolute joints. Furthermore, the interaction of the cable with the pulley is modeled. The bond graph approach is utilized for modeling and the obtained simulation results are discussed. The model is validated by comparing its results with the *catenary* cable model of the CDPR.

Keywords: cable-driven parallel robots, cable mass and elasticity, discretized catenary model, bond graph.

1 INTRODUCTION

Cable-driven parallel robot (CDPR) belongs to the class of parallel robots where the rigid links are replaced by flexible cables. This modification provides certain advantages such as small inertia, high payload to weight ratio and large workspace. Owing to these advantages, the CDPRs have been used in many applications such as large-scale telescopes (Li and Pan 2016), stadium video camera systems (Cone 1985), large-scale motion-simulators (Miermeister et al. 2016), to name a few.

On the other hand, the cables encounter certain challenges in kinematics, statics, and dynamics of CDPRs because of their flexibility. Modeling of the cables becomes very challenging when one considers cable mass, elasticity, flexural stiffness as well as damping into account. This is generally required for large-scale robots where the mass and elasticity of the cable is non-negligible and can significantly affect the statics (Chawla et al. 2021a) as well as dynamic response (Yuan, Courteille, and Deblaise 2015) of the CDPR.

Most of the work in the literature assume the cables to be *ideal* (i.e., massless and inelastic cable) while modeling the CDPRs (Khosravi and Taghirad 2014b; Shang et al. 2019). This assumption makes the modeling approach quite simple and easy to use. Since cables can only pull and not push, this modeling approach assumes the cable to be taunt by putting unilateral tension constraints in the controller design. In practice, the *ideal* cable model is only suitable for small-scale CDPRs (with cables of negligible mass) operating at small speeds and accelerations.

From the last decade, the *elastic* cable model has become a popular choice among researchers for dynamic analysis and controller design of CDPR. This model assumes the cables to be massless elastic springs to account for the vibrations induced due to elasticity in the cable (Diao and Ma

2009; Khosravi and Taghirad 2014a). This model is well suited for small-scale CDPRs with taunt cables. However, for large scale CDPRs, the mass of the cable can significantly affect the dynamics of the CDPRs. In addition, the transversal vibrations in this case would be significant which are ignored in *elastic* cable model.

To account for the cable mass, the *catenary* cable model (cable with mass and elasticity) (Irvine 1981; Kozak, Zhou, and Wang 2006) has been used for dynamic analysis of large-scale CDPRs (Zi et al. 2008). In addition, this model has been extensively used for the kineto-static analysis in the literature (Chawla et al. 2021b). However, the model assumes that the motion of the robot is quasi-static. This assumption can be considered valid for some of the applications of large-scale CDPRs (such as 3D printing (Chawla et al. 2021c) and telescope) but not all. On the other hand, the model ignores flexural stiffness which is non-negligible for thick cables.

A very limited volume of work in the literature focuses on the comprehensive dynamic model of CDPR. They are either based on finite element method (Du et al. 2012; Cui et al. 2015) or lumped mass approach (Collard, Lamaury, and Gouttefarde 2011; Caverly, Member, and Forbes 2014; Mamidi and Bandyopadhyay 2021). Most of these models do not consider all the phenomena's (such as cable mass, elasticity, flexural stiffness, flexural damping and pulley) altogether. Another major challenge is to model the change in cable length which is generally required to simulate the motion of CDPR. This challenge is addressed either by using finite element of variable length (Cui et al. 2015) or by increasing/reducing the number of elements/segments of the cable (Collard, Lamaury, and Gouttefarde 2011). Both approaches are computationally intense and are difficult to incorporate in simulation due to time-varying initial conditions for each element.

In this work, we propose a comprehensive dynamic model of CDPR by considering the effect of cable mass, elasticity, flexural stiffness, and flexural damping altogether. In addition, we also present a dynamic model for cable-pulley interaction which can be used to analyze the change in cable lengths without changing the number of segments or changing segment length. A bond graph approach is used to model and simulate the whole system. A planar CDPR with 2 cables is considered for simulation. The obtained results are validated with the kineto-static analysis of *catenary* cable model.

This paper is organized as follows: In Section 2, the dynamic modeling of cable, cable-pulley interaction and the whole CDPR is presented. The results and discussions for a planar CDPR is discussed in Section 3. Finally, in Section 4, the conclusions are drawn.

2 DYNAMIC MODELING OF A CABLE-DRIVEN PARALLEL ROBOT

2.1 Dynamic Modeling of a Cable

In this work, the cable is modeled as a series of spring-mass-damper systems connected by a revolute joint, as shown in Figure 1. Each revolute joint can have a stiffness and damping coefficient to account for the stiffness and damping characteristics of the cable due to bending. For illustration, consider a cable of radius r, unstrained length l_0, unstrained cross-sectional area A_0, unstrained linear density ρ_0, normal damping material constant d_n and elastic modulus E. The total mass m of the cable can be obtained as $m = \rho_0 l_0$.

For the purpose of dynamic modeling, the cable is discretized into n spring-mass-damper system of equal lengths. The length $l_{0_i} = \frac{l_0}{n}$ represents the unstrained length of i^{th} spring-mass-damper system with spring stiffness k_i and viscous damping coefficient c_i. Each spring-mass-damper system is connected to the corresponding spring-mass-damper system by a revolute joint with a joint angle of θ_i with respect to x axis and considered positive in a clockwise direction. The parameters k_{θ_i} and c_{θ_i} represents the stiffness and viscous damping coefficients of i^{th} revolute joint. One end of the cable is hinged to the origin of the coordinate frame while the other end is free. The gravitational acceleration is acting in the negative z axis of the coordinate frame. The cable is assumed to lie in a vertical plane; therefore, the proposed model is planar in nature. However, on replacing revolute joints with u-joints, the model can be easily modified to be a spatial model.

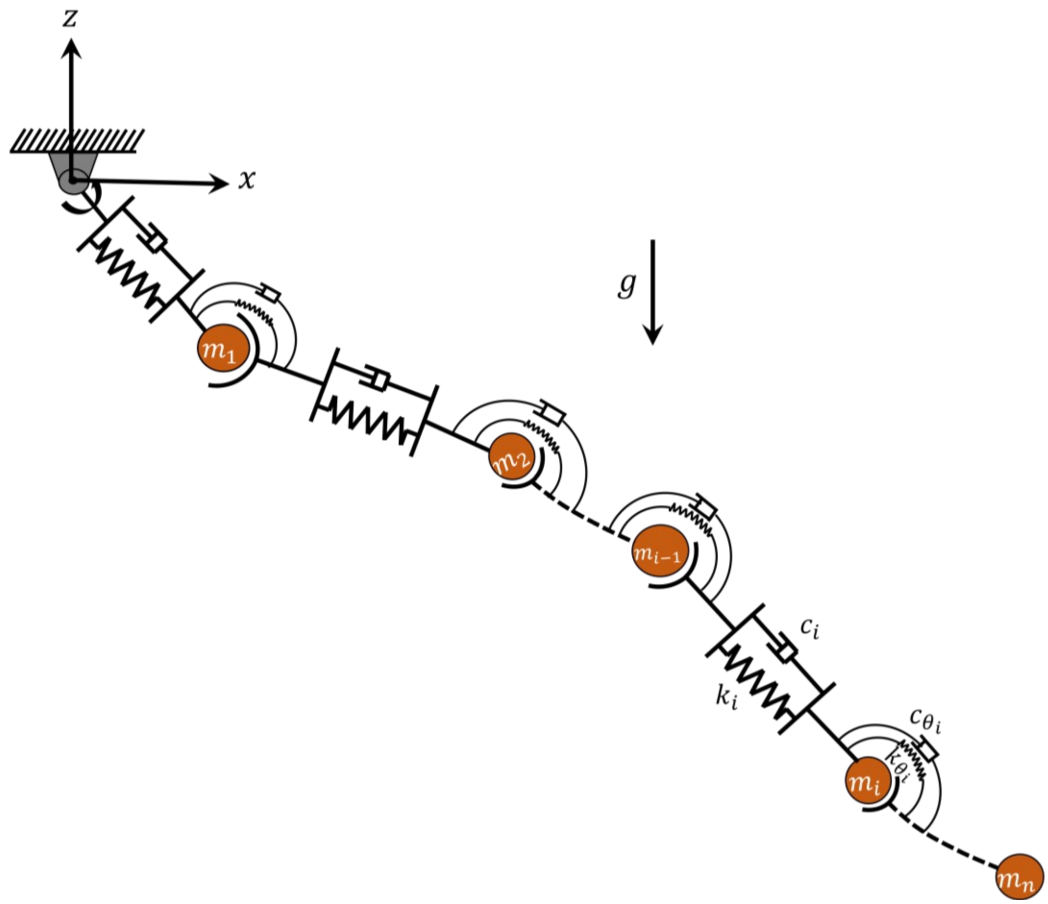

Figure 1: Schematic diagram of a cable

The coefficient of stiffness and damping can be represented via beam-equivalence theory (Wittbrodt, Edmund, Adamiec-Wójcik, and Wojciech 2007) as:

$$k_i = \frac{EA_0}{l_{0_i}}, c_i = \frac{d_n A_0}{l_{0_i}}, k_{\theta_i} = \frac{EJ}{l_{0_i}}, c_{\theta_i} = \frac{d_n J}{l_{0_i}},$$

where $J = \frac{\pi r^4}{4}$ represents the second moment of area.

Let x_i and z_i represents the position of mass m_i of the spring-mass-damper system representing the cable. The position of mass m_i must satisfy the following kinematic relation:

$$x_i = x_{i-1} + l_i \cos\theta_i, \tag{1}$$

$$z_i = z_{i-1} - l_i \sin\theta_i, \tag{2}$$

where x_{i-1} and z_{i-1} represents the position of mass m_{i-1} and l_i represents the strained length of the i^{th} element which is the summation of unstrained length l_{0_i} and elastic elongation Δl_i. The differentiation of (1) and (2) with respect to time t yields:

$$\dot{x}_i = \dot{x}_{i-1} + \dot{l}_i \cos\theta_i - l_i \sin\theta_i \dot{\theta}_i, \tag{3}$$

$$\dot{z}_i = \dot{z}_{i-1} - \dot{l}_i \sin\theta_i - l_i \cos\theta_i \dot{\theta}_i. \tag{4}$$

Rearranging (3) and (4) gives:

$$l_i \sin\theta_i \dot{\theta}_i = \dot{x}_{i-1} - \dot{x}_i + \dot{l}_i \cos\theta_i, \tag{5}$$

$$l_i \cos\theta_i \dot{\theta}_i = \dot{z}_{i-1} - \dot{z}_i - \dot{l}_i \sin\theta_i. \tag{6}$$

Multiplying (5) by $\sin\theta_i$ and (6) by $\cos\theta_i$ and adding yields:

$$l_i \dot{\theta}_i = (\dot{x}_{i-1} - \dot{x}_i) \sin\theta_i + (\dot{z}_{i-1} - \dot{z}_i) \cos\theta_i. \tag{7}$$

Substituting $\cos\theta_i$ and $\sin\theta_i$ form (1) and (2), respectively in (7) gives:

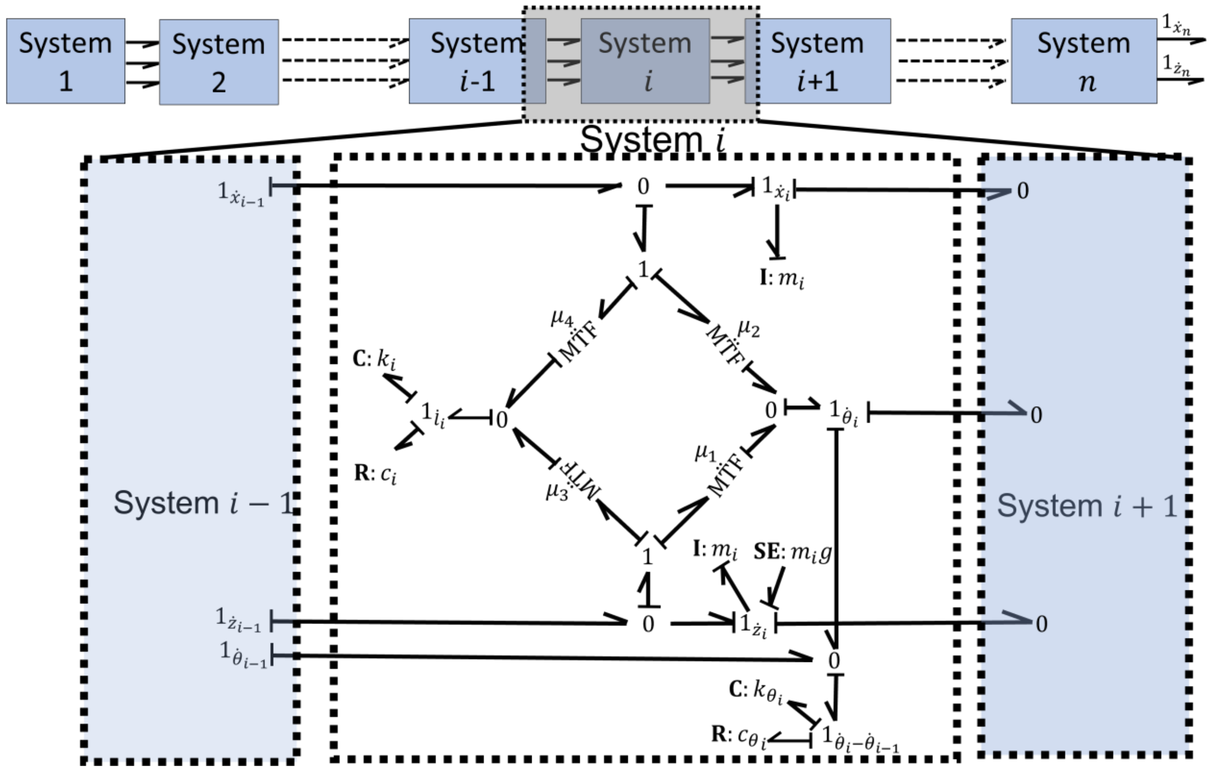

Figure 2: Bond graph model of a cable

$$l_i\dot{\theta}_i = (\dot{x}_{i-1} - \dot{x}_i)\frac{(z_{i-1}-z_i)}{l_i} + (\dot{z}_{i-1} - \dot{z}_i)\frac{(x_i-x_{i-1})}{l_i}. \quad (8)$$

Rewriting (8) provides:

$$\dot{\theta}_i = \frac{(z_i-z_{i-1})}{l_i^2}(\dot{x}_i - \dot{x}_{i-1}) - \frac{(x_i-x_{i-1})}{l_i^2}(\dot{z}_i - \dot{z}_{i-1}). \quad (9)$$

Equation (9) gives the kinematic relation for $\dot{\theta}_i$. In a similar way, the kinematic relation for $\dot{l}_i$ can be derived using the following kinematic relation for strained length l_i:

$$l_i = \sqrt{(x_i - x_{i-1})^2 + (z_i - z_{i-1})^2}. \quad (10)$$

Squaring both sides yield:

$$l_i^2 = (x_i - x_{i-1})^2 + (z_i - z_{i-1})^2. \quad (11)$$

Differentiating (11) with respect to time t gives:

$$2\, l_i\dot{l}_i = 2(x_i - x_{i-1})(\dot{x}_i - \dot{x}_{i-1}) + 2(z_i - z_{i-1})(\dot{z}_i - \dot{z}_{i-1}), \quad (12)$$

$$\dot{l}_i = \frac{(x_i-x_{i-1})}{l_i}(\dot{x}_i - \dot{x}_{i-1}) + \frac{(z_i-z_{i-1})}{l_i}(\dot{z}_i - \dot{z}_{i-1}). \quad (13)$$

Therefore, using the kinematic relation for $\dot{\theta}_i$ and $\dot{l}_i$, the bond graph of the system is prepared, as shown in Figure 2. The transformer moduli applied in the bond graph are given in Table 1.

Table 1: Transformer Moduli for Bond Graph Modeling

$\mu_1 = \frac{-(x_i - x_{i-1})}{l_i}$	$\mu_2 = \frac{-(z_i - z_{i-1})}{l_i}$
$\mu_3 = \frac{-(z_i - z_{i-1})}{l_i^2}$	$\mu_4 = \frac{(x_i - x_{i-1})}{l_i^2}$

The cable is discretized into n spring-mass-damper system attached by a revolute joint. Each system (except first and last) is connected to each other via three bonds. These three bonds transfer the energy from one system to another. The bond graph model of i^{th} spring-mass-damper system is descriptively shown in Figure 2. The i^{th} system is connected to $i-1^{th}$ system vie three bonds which transfer flow information from $i-1^{th}$ system to i^{th} system. The i^{th} system is also connected to

$i+1^{th}$ system via bonds to transfer flow information to $i+1^{th}$ system. A source of effort is applied on $1_{\dot{z}_i}$ representing the gravitational force due to mass m_i, where $g = -9.8\frac{\text{m}}{\text{s}^2}$ represents gravitational acceleration. Additionally, the inertia element is applied to $1_{\dot{x}_i}$ and $1_{\dot{z}_i}$. A stiffness element with k_i as spring stiffness and resistance element with c_i as resistance is connected to $1_{\dot{l}_i}$ to account for the elastic stiffness and longitudinal damping. The effort for the stiffness element is proportional to the elastic elongation Δl_i of i^{th} system/element.

The stiffness element with k_{θ_i} as rotational stiffness and resistive element with c_{θ_i} as viscous damping coefficient is connected to $1_{\dot{\theta}_i - \dot{\theta}_{i-1}}$ to account for the bending stiffness and transversal damping of the cable, respectively. The effort corresponding to bending stiffness element is proportional to the difference in the joint angle between the previous system joint angle θ_{i-1} and considered system joint angle θ_i. In case the other end of cable is holding a point mass M, the inertia element and source of effort of n^{th} system can be updated to include the point mass M.

2.2 Dynamic Modeling of a Cable-Pulley Interaction

The pulley is modeled as a spring of high stiffness and a damper (as shown in Figure 3) which apply a resistive force on the cable only when the cable is inside the boundary of the object. This implies that the force is exerted on the cable if any of the point mass of the spring-mass-damper system is inside the boundary or comes in contact with the boundary of a pulley. This is checked by measuring the distance between the center of a pulley (x_p, z_p) and the coordinates of the mass (x_i, z_i) (i.e., $d_{p_i} = \sqrt{(x_p - x_i)^2 + (z_p - z_i)^2}$) and applying a condition when the distance is less than the radius of a pulley r_p. In bond graph, the cable-pulley interaction is modeled by inserting a modulated source of effort (MSE) on $1_{\dot{x}_i}$ and $1_{\dot{z}_i}$ junction of i^{th} system for $i = 1,2,\dots,n$ in Figure 2. The effort for MSE corresponding to $1_{\dot{x}_i}$ and $1_{\dot{z}_i}$, respectively is given by (14) and (15). The parameters k_p and c_p represent the spring stiffness and damping coefficient of pulley, respectively.

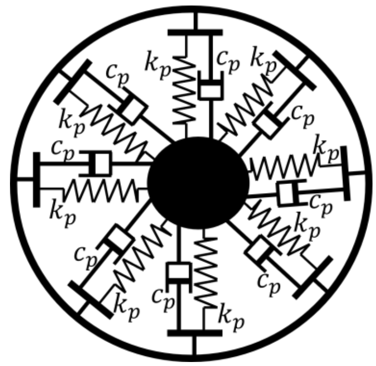

Figure 3: Schematic diagram of a pulley

$$e_{\dot{x}_i} = \begin{cases} k_p(x_p - x_i) - c_p\dot{x}_i \text{ ; if } d_{p_i} \le r_p \\ 0 \quad\quad\quad\quad\quad\quad\quad\quad \text{; otherwise} \end{cases} \tag{14}$$

$$e_{\dot{z}_i} = \begin{cases} k_p(z_p - z_i) - c_p\dot{z}_i \text{ ; if } d_{p_i} \le r_p \\ 0 \quad\quad\quad\quad\quad\quad\quad\quad \text{; otherwise} \end{cases} \tag{15}$$

2.3 Dynamic Modeling of a Cable-Driven Parallel Robot

Figure 4 shows the schematic diagram of a general cable driven parallel robot. It consists of the cables connected in parallel to the mobile platform at one end and to the winches (via pulleys) at the other end. The motion of the mobile platform is controlled by changing the length of the cables with the application of winches. For the dynamic analysis of this system, it is important to model the cables as well as pulleys which is discussed comprehensively in the previous subsections.

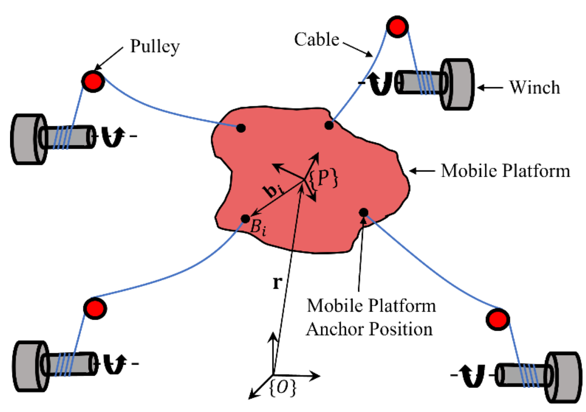

Figure 4: Schematic diagram of CDPR

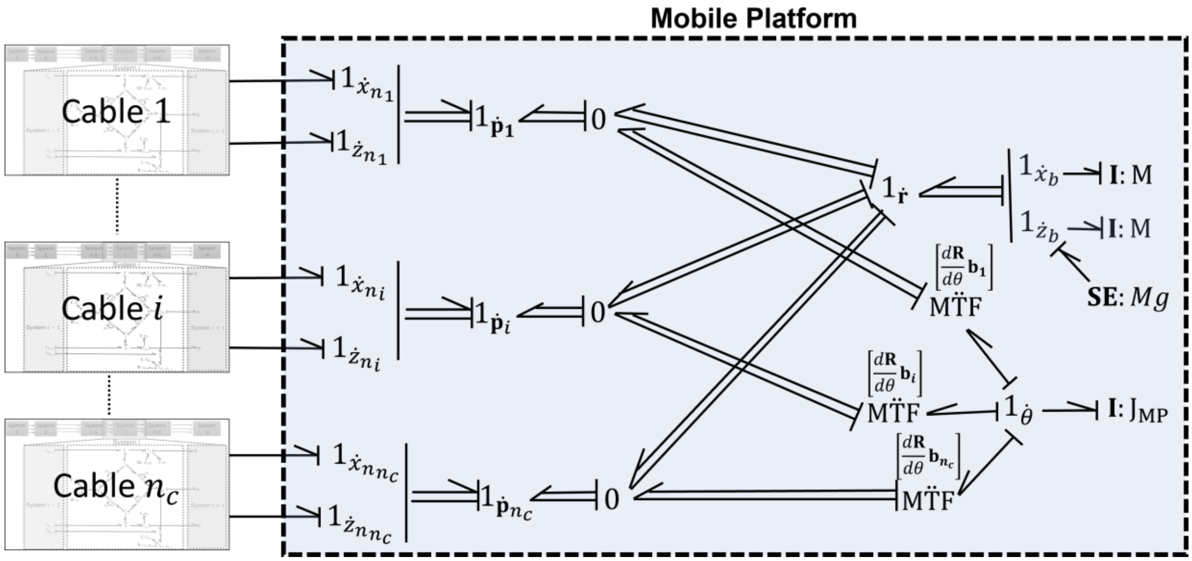

Figure 5: Bond graph model of a CDPR

Let $\{O\}$ represents the global coordinate frame and $\{P\}$ denotes the local coordinate frame attached to the center of mass of the mobile platform. The vector $\mathbf{r} = [x_b \; z_b]^T$ represents the position of the local coordinate frame $\{P\}$ in the global coordinate frame $\{O\}$. The position vector $\mathbf{b}_i$ symbolizes the position of i^{th} cable anchor point with respect to the local frame $\{P\}$. The rotation matrix $\mathbf{R}$ characterizes the orientation of the mobile platform. The cable anchor point corresponding to global frame $\{O\}$ can be given by:

$$\mathbf{p}_i = \mathbf{r} + \mathbf{R}\mathbf{b}_i \tag{16}$$

where the rotation matrix $\mathbf{R}$ for the rotation of mobile platform by angle θ along y-axis can be represented as:

$$\mathbf{R} = \begin{bmatrix} \cos\theta & -\sin\theta \\ \sin\theta & \cos\theta \end{bmatrix} \tag{17}$$

The velocity of the cable anchor point can be obtained by differentiating (16) with respect to time t as:

$$\dot{\mathbf{p}}_i = \dot{\mathbf{r}} + \frac{d\mathbf{R}}{d\theta}\dot{\theta}\,\mathbf{b}_i \tag{18}$$

Equation (18) can be used to develop the bond graph model of the mobile platform, as shown in Figure 5. The junction $1_{\dot{x}_b}$ and $1_{\dot{z}_b}$ represents the velocity of the center of mass of the mobile platform in x and z direction, respectively. For a cable-driven parallel robot, where n_c number of cables are connected in parallel to a single mobile platform, the output of last spring-mass-damper system for all the cables should be connected to the bond graph model of a mobile-platform. This means that the junction $1_{\dot{x}_{n_i}}$ and $1_{\dot{z}_{n_i}}$ should be connected to mobile platform where $i = 1,2,\dots,n_c$. The parameter M and J_{MP} represents the mass and moment of inertia of the mobile platform. The dynamic equations for the bond graph can be obtained using 20-Sim software. After obtaining the dynamic equation, the dynamics of CDPR can be simulated by defining the initial conditions and parameters of the robot.

3 RESULTS AND DISCUSSION

In this section, the simulation results for the proposed dynamic model of CDPR are presented. A stainless-steel cable 18 × 7 of 10 mm diameter is used for the simulation. This cable has been used in CoGiRo robot and the parameters of the CDPR are given in Table 2. The parameters of the cable are adopted from (Merlet 2016) except the parameter 4 which is taken from (Baklouti et al. 2017).

A suspended CDPR with 2 cables is considered for simulation in this paper. The pulley corresponding to cable 1 is fixed at $[x_{p_1}, z_{p_1}] = [-1.75, 0]$ m corresponding to global reference frame. The pulley for cable 2 is fixed at $[x_{p_2}, z_{p_2}] = [1.75, 0]$ m. A rectangular mobile platform of length $l_p = 0.3$ m and height $h_p = 0.2$ m is considered. The center of mass of the mobile platform is considered at the geometrical center of the rectangular platform. The cable anchor point corresponding to frame $\{P\}$ are given by $b_1 = \left[-\frac{l_p}{2}, \frac{h_p}{2}\right]^T$ and $b_2 = \left[\frac{l_p}{2}, \frac{h_p}{2}\right]^T$. At initial position, the mobile platform is at $\mathbf{r} = [0, -2]$ m and zero orientation (i.e., $\theta = 0°$). The initial configuration of both the cables is obtained using the inverse kinematics for *ideal* cables, as shown in Figure 6 (a). For simulation, the free end of both the cables is pulled downward to achieve a circular motion of the mobile platform. Therefore, the reference position $\mathbf{r}_{ref}$ of the mobile platform is given by:

$$\mathbf{r}_{ref} = \begin{bmatrix} 0.4 \sin 1.5t \\ -1.6 - 0.4 \cos 1.5t \end{bmatrix} \tag{19}$$

The orientation of the reference trajectory in considered to be zero. The velocity of the cables at the free end with respect to the reference velocity of the mobile platform is obtained by using inverse kinematics for *ideal* cables (Lenaričič and Husty 2012). This velocity is applied as a source of flow in negative z-axis to the first element of each cable. The animation of the CDPR at different time instants is shown in Figure 6. The readers may refer https://youtu.be/3ahQHTX8ahI to watch the animation of the results shown in Figure 6.

Table 2: Parameters of CDPR

Symbol	Description	Value
r	Radius of the cable	5 mm
l_0	Unstrained length of the cable	3.75 m
ρ_0	Linear density of the cable	0.35 kg/m
d_n	Normal damping material constant	10^9 Ns/m^2
E	Modulus of elasticity	10^9 N/m^2
n	Number of elements	15
k_i	Stiffness of i_{th} element	3.14×10^5 N/m
c_i	Viscous damping coefficient of i_{th} element	3.14×10^5 Ns/m
k_{θ_i}	Stiffness of i_{th} revolute joint	1.96 Nm/rad
c_{θ_i}	Viscous damping coefficient of i_{th} revolute joint	1.96 Nms/rad
k_p	Stiffness of pulley	10^7 N/m
c_p	Viscous damping coefficient for cable-pulley interaction	10 Ns/m
r_p	Radius of pulley	0.25 m
M	Mass of the mobile platform	2.5 kg
J_{MP}	Moment of inertia of the mobile platform	0.0271 kg m^2

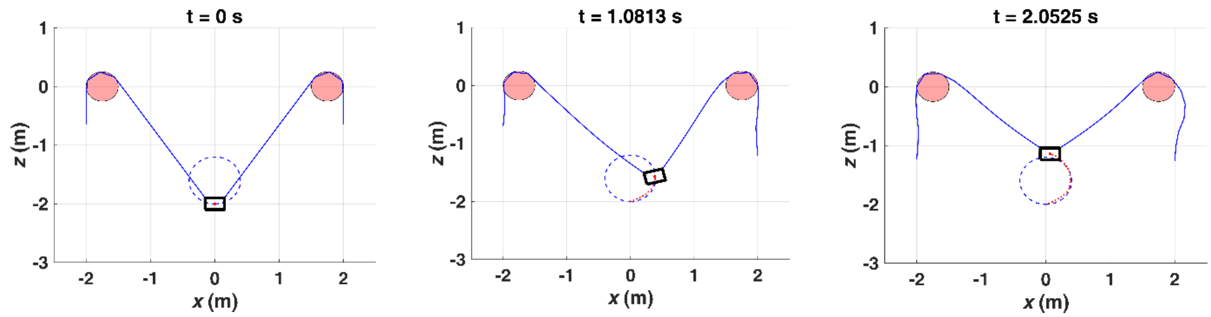

Figure 6: Simulation of CDPR at different time instants

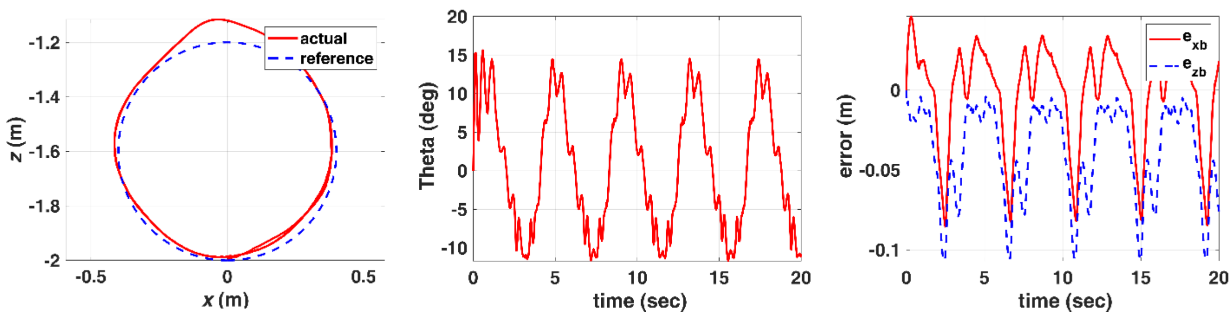

(a) Contour Plot (b) Platform Orientation (c) Position Error

Figure 7: Simulation response for the motion of the mobile platform

The results show that the mobile platform is gradually moving along a circular trajectory with the increase in time. The sagging of the cables can be clearly seen in Figure 6 (b) and 6 (c). The results can be closely visualized by Figure 7 (a) which shows the trajectory taken by the mobile platform in comparison to the desired trajectory. On the other hand, Figure 7 (b) shows the orientation of the mobile platform while following the trajectory. The position error of the actual trajectory with respect to the reference trajectory can be seen in Figure 7 (c). A maximum position error of 8.5 cm and 11 cm is observed in x and z direction, respectively. On the other hand, a maximum error of 15 ° is observed in the orientation of the platform. A negative error in the z direction is observed throughout the trajectory. This is because of the large sagging in the cables. In general, the error is because of the mass and elastic elongation of the cable which are ignored while obtaining the inverse kinematics using *ideal* cable model. The presented error also shows that if a joint-space controller is designed based on the inverse kinematics of *ideal* cable model, the proposed system will encounter at least 11 cm error. This shows the importance of the proposed dynamic model in simulating the accuracy of the CDPR.

The *catenary* cable model (Kozak, Zhou, and Wang 2006) of the CDPR which is observed to be in good agreement with the experimental results is utilized for the validation of the proposed model. This *catenary* model considers the cable mass and elasticity but ignores the flexural stiffness for the analysis (Kozak, Zhou, and Wang 2006). At the initial configuration, the cable 1 and cable 2 are straight and are making an angle of 45° and 135°, respectively with respect to x-axis. In this case, the mobile platform of small point mass ($M = 1$ kg) is considered to compare the results at large sagging. The proposed model is simulated until a static state is reached. The static state of the CDPR using the proposed model is shown in Figure 8. Similarly, the cable profiles are obtained by doing the inverse kineto-static analysis for the *catenary* cable model, as shown by dotted red color in Figure 8. The cable profiles for the proposed model are observed to be in close proximity with the *catenary* cable model. A minor difference of 0.8 mm is observed in the cable lengths of both models. In addition, a relatively small bending in the cable is observed in the proposed model as compared to *catenary* cable model due to the ignored flexural stiffness in the *catenary* cable model.

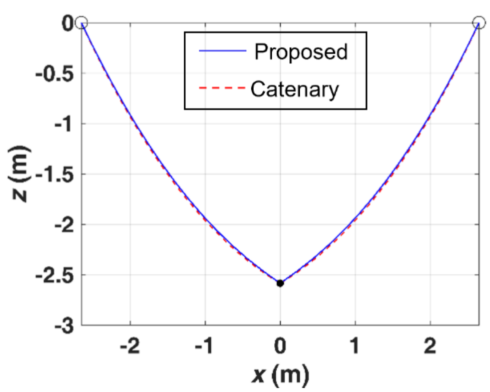

Figure 8: Comparison of the proposed model with the *catenary* cable model

4 CONCLUSION

In this paper, a comprehensive dynamic model of the cable-driven parallel robot is proposed. This model considers the cable mass, elasticity, flexural stiffness, and flexural damping for the dynamic modeling of the CDPR. The proposed dynamic model considers the cable to be a series of spring-mass-damper systems connected by the revolute joints. In addition, the dynamic model for the interaction of the cable with the pulley is also presented. The bond graph approach is utilized for modeling and simulation of the proposed model. A suspended CDPR with 2 cables is considered for simulation. The velocity of the cables with respect to the reference velocity of the mobile platform is obtained by using inverse kinematics for the *ideal* cable model. The results show a significant error in the actual trajectory of the mobile platform which marks the importance of the proposed dynamic model in simulating the accuracy of the CDPR. The validation of the proposed model is provided by comparing its results with the *catenary* cable model. The obtained results are encouraging and motivates us to extend the model to spatial configurations that can be utilized for the dynamic analysis of complex CDPRs in the future.

REFERENCES

Baklouti, Sana, Eric Courteille, Stéphane Caro, and Mohamed Dkhil. 2017. “Dynamic and Oscillatory Motions of Cable-Driven Parallel Robots Based on a Nonlinear Cable Tension Model.” *Journal of Mechanisms and Robotics* 9 (6): 061014.

Caverly, Ryan James, Student Member, and James Richard Forbes. 2014. “Dynamic Modeling and Noncollocated Control of a Flexible Planar Cable-Driven Manipulator.” *IEEE Transactions on Robotics* 30 (6): 1386–97.

Chawla, Ishan, P. M. Pathak, Leila Notash, A. K. Samantaray, Qingguo Li, and U. K. Sharma. 2021a. “Effect of Selection Criterion on the Kineto-Static Solution of a Redundant Cable-Driven Parallel Robot Considering Cable Mass and Elasticity.” *Mechanism and Machine Theory* 156: 104175.

———. 2021b. “Neural Network-Based Inverse Kineto-Static Analysis of Cable-Driven Parallel Robot Considering Cable Mass and Elasticity.” In *International Conference on Cable-Driven Parallel Robots*, 50–62. Springer.

———. 2021c. “Workspace Analysis and Design of Large-Scale Cable-Driven Printing Robot Considering Cable Mass and Mobile Platform Orientation.” *Mechanism and Machine Theory* 165: 104426.

Collard, Jean-François, Johann Lamaury, and Marc Gouttefarde. 2011. “Dynamics Modelling of Large Suspended Parallel Cable-Driven Robots Multibody Model.” In *Multibody Dynamics, ECCOMAS Thematic Conference*, 1–13.

Cone, Lawrence L. 1985. “Skycam-an Aerial Robotic Camera System.” *Byte*, 1985.

Cui, Chuanzhen, Jingli Du, Hong Bao, and Yuanying Qiu. 2015. “Dynamic Analysis of Cable-Driven Parallel Manipulators Using a Variable Length Finite Element.” *Journal of Computational and Nonlinear Dynamics* 10

(1): 011013.

Diao, Xiumin, and Ou Ma. 2009. "Vibration Analysis of Cable-Driven Parallel Manipulators." *Multibody System Dynamics* 21: 347–60.

Du, Jingli, Hong Bao, Chuanzhen Cui, and Dongwu Yang. 2012. "Dynamic Analysis of Cable-Driven Parallel Manipulators with Time-Varying Cable Lengths." *Finite Elements in Analysis and Design* 48 (1): 1392–99.

Irvine, H. Max. 1981. "Cable Structures." Cambridge: The MIT Press.

Khosravi, Mohammad A, and Hamid D Taghirad. 2014a. "Dynamic Modeling and Control of Parallel Robots with Elastic Cables : Singular Perturbation Approach." *IEEE Transactions on Robotics* 30 (3): 694–704.

———. 2014b. "Robust PID Control of Fully-Constrained Cable Driven Parallel Robots." *Mechatronics* 24: 87–97.

Kozak, Kris, Qian Zhou, and Jinsong Wang. 2006. "Static Analysis of Cable-Driven Manipulators with Non-Negligible Cable Mass." *IEEE Transactions on Robotics* 22 (3): 425–33.

Lenaričič, Jadran, and Manfred Husty. 2012. "Influence of Pulley Kinematics on Cable-Driven Parallel Robots." In *Latest Advances in Robot Kinematics*, 197–204. Springer.

Li, Di, and Zhichen Pan. 2016. "The Five-Hundred-Meter Aperture Spherical Radio Telescope Project." *Radio Science* 51 (7): 1060–64.

Mamidi, Teja Krishna, and Sandipan Bandyopadhyay. 2021. "Forward Dynamic Analyses of Cable-Driven Parallel Robots with Constant Input with Applications to Their Kinetostatic Problems." *Mechanism and Machine Theory* 163: 104381.

Merlet, J. P. 2016. "A Generic Numerical Continuation Scheme for Solving the Direct Kinematics of Cable-Driven Parallel Robot with Deformable Cables." In *IEEE International Conference on Intelligent Robots and Systems*, 4337–43. IEEE.

Miermeister, Philipp, Maria Lächele, Rainer Boss, Carlo Masone, Christian Schenk, Joachim Tesch, Michael Kerger, Harald Teufel, Andreas Pott, and Heinrich H. Bülthoff. 2016. "The CableRobot Simulator Large Scale Motion Platform Based on Cable Robot Technology." In *IEEE International Conference on Intelligent Robots and Systems*, 3024–29.

Shang, Weiwei, Bingyuan Zhang, Bin Zhang, and Fei Zhang. 2019. "Synchronization Control in the Cable Space for Cable-Driven Parallel Robots." *IEEE Transactions on Industrial Electronics* 66 (6): 4544–54.

Wittbrodt, Edmund, Iwona Adamiec-Wójcik, and Stanislaw Wojciech. 2007. *Dynamics of Flexible Multibody Systems: Rigid Finite Element Method*. Springer Science & Business Media.

Yuan, Han, Eric Courteille, and Dominique Deblaise. 2015. "Static and Dynamic Stiffness Analyses of Cable-Driven Parallel Robots with Non-Negligible Cable Mass and Elasticity." *Mechanism and Machine Theory* 85: 64–81.

Zi, B., B. Y. Duan, J. L. Du, and H. Bao. 2008. "Dynamic Modeling and Active Control of a Cable-Suspended Parallel Robot." *Mechatronics* 18 (1): 1–12.

AUTHOR BIOGRAPHIES

ISHAN CHAWLA is an Senior Research Fellow in the Mechanical & Industrial Engineering Department of Indian Institute of Technology Roorkee. He received his B.Tech. degree in Mechanical Engineering from Punjabi University, Patiala in 2015 and M.E. in CAD/CAM from Thapar University, Patiala in 2017. He is an active researcher on Cable-Driven Parallel Robots. His areas of interest include Robotics, Neural Networks, Underactuated Systems, Dynamic Modeling and Control. His email address is ichawla@me.iitr.ac.in.

PUSHPARAJ MANI PATHAK is currently a Professor at Indian Institute of Technology Roorkee, India. He graduated from National Institute of Technology Calicut, India in 1988 in Mechanical Engineering. He completed his M. Tech in Solid Mechanics and Design from Indian Institute of Technology Kanpur in 1998. Later he was awarded the PhD degree from IIT Kharagpur in 2005. His areas of research are Robotics, Dynamics, Control, and Bond Graph Modelling. He is serving in Mechanical and Industrial Engineering Department, IIT Roorkee since 2006. He has co-authored one book on Intelligent Mechatronic Systems: Modeling, Control and Diagnosis published by Springer, London. He is a Member of International Federation for the Promotion of Mechanism and Machine Science (IFToMM) Technical committee for Multi Body Dynamics. His email address is pushparaj.pathak@me.iitr.ac.in.

ARUN KUMAR SAMANTARAY is a full Professor and Incharge of Systems, Dynamics and Control Laboratory in Mechanical Engineering Department of IIT Kharagpur. He received BTech degree in 1989 from CET Bhubaneswar, and MTech degree in Machine Dynamics and PhD in Mechanical Engineering from IIT Kharagpur in the years 1991 and 1996, respectively. He worked as a Project Manager for HighTech consultants from 1996 to 2000 and as a CNRS researcher at Université Lille 1: Sciences et Technologies, France, from 2001 to 2004. He has authored three books and many journal articles. He is also a consultant to various industries. His research interests include Robotics, Systems and Control, Fault Diagnosis, Automation, Non-Linear Mechanics, Robotics, Rotor Dynamics and Vehicle Dynamics. His email address is samantaray@mech.iitkgp.ernet.in.